AD_____

Award Number: W81XWH-09-1-0303

TITLE: Development of a Nanotechnology Platform for Prostate Cancer Gene Therapy

PRINCIPAL INVESTIGATOR: Arash Hatefi, Ph.D.

CONTRACTING ORGANIZATION: Rutgers, The State University of New Jersey
New Brunswick, NJ 08901

REPORT DATE: July 201H

TYPE OF REPORT: Ø§ ¾|

PREPARED FOR: U.S. Army Medical Research and Materiel Command
Fort Detrick, Maryland 21702-5012

DISTRIBUTION STATEMENT: Approved for Public Release;
Distribution Unlimited

REPORT DOCUMENTATION PAGE

1. REPORT DATE	2. REPORT TYPE	3. DATES COVERED
July 201H	Œ} æ¢	1 July 20€J – 30 June 201H

4. TITLE AND SUBTITLE

Development of a Nanotechnology Platform for Prostate Cancer Gene Therapy

5a. CONTRACT NUMBER

5b. GRANT NUMBER
W81XWH-09-1-0303

5c. PROGRAM ELEMENT NUMBER

6. AUTHOR(S)

Arash Hatefi, Ph.D.

5d. PROJECT NUMBER

5e. TASK NUMBER

5f. WORK UNIT NUMBER

E-Mail: ahatefi@pharmacy.rutgers.edu

7. PERFORMING ORGANIZATION NAME(S) AND ADDRESS(ES)

Rutgers, The State University of New Jersey
New Brunswick, NJ 08901

8. PERFORMING ORGANIZATION REPORT NUMBER

9. SPONSORING / MONITORING AGENCY NAME(S) AND ADDRESS(ES)
U.S. Army Medical Research and Materiel Command
Fort Detrick, Maryland 21702-5012

10. SPONSOR/MONITOR'S ACRONYM(S)

11. SPONSOR/MONITOR'S REPORT NUMBER(S)

12. DISTRIBUTION / AVAILABILITY STATEMENT
Approved for Public Release; Distribution Unlimited

13. SUPPLEMENTARY NOTES

14. ABSTRACT
The objective of this research is to design and develop a nanocarrier that is able to evade the immune system, circulate in the blood stream, find its target prostate cancer cells, and transfer therapeutic genes into prostate cancer cells efficiently. The gene carrier is composed of: a) histone H2A peptide to condense pDNA into nano-size particles, b) a PC-3 specific targeting motif (TM) to target prostate cancer cells, c) an endosomolytic motif to disrupt endosome membrane, and d) a nuclear localization signal (NLS) to actively translocate pDNA towards the nucleus of cancer cells. The gene delivery system was synthesized in E.coli. The vector was then complexed with plasmid DNA (pDNA) to form stable nanoparticles with sizes below 100nm. The nanoparticles were used to deliver reporter genes (pEGFP) to target PC-3 prostate cancer cells and RWPE-1 normal epithelial prostate cells. The induction of immune response by the vector was studied in BALB/c immune-competent mice. The results demonstrated that the gene delivery system is able to target and efficiently transfect PC-3 cancer cells with minimum cross-reactivity with normal epithelial prostate cells. An animal protocol was prepared and approved by IACUC and DOD ACURO. The immunogenicity studies showed that the vector does not induce production IgG or IgM after repeated systemic injection.

15. SUBJECT TERMS
Nanocarriers, non-immunogenic, PC-3 prostate cancer targeting, vector development

16. SECURITY CLASSIFICATION OF:			17. LIMITATION OF ABSTRACT	18. NUMBER OF PAGES	19a. NAME OF RESPONSIBLE PERSON USAMRMC
a. REPORT	b. ABSTRACT	c. THIS PAGE			19b. TELEPHONE NUMBER *(include area code)*
U	U	U	UU	Gì	

Table of Contents

<u>Introduction</u>

A major obstacle to improving patients' survival with advanced prostate cancer is progression of the cancer to androgen-independence. Therefore, methods such as gene therapy capable of delay or stop this progression may have a significant impact on improving patients' health. However, many challenges lie ahead for gene therapy, including improving DNA transfer efficiency to cancer cells, enhancing levels of gene expression, and overcoming immune responses. **The overall objective** of this research is to design and develop a nanocarrier that is able to evade the immune system, circulate in the blood stream, find its target prostate cancer cells, and transfer therapeutic genes into prostate cancer cells efficiently. The gene carrier is composed of: a) histone H2A peptide (H2A) to condense plasmid DNA (pDNA) into nano-size particles (nanocarriers), b) a PC-3 specific targeting motif (TM) to target prostate cancer cells, c) an endosome disrupting motif (EDM) to disrupt endosome membranes and facilitate escape of the cargo into the cytosol, and d) a nuclear localization signal (NLS) to actively translocate pDNA towards the nucleus of cancer cells. An elastin like polymer (ELP) has also been engineered in the vector structure to provide a hydrophilic shield and protect the vector/pDNA complex in the blood stream from the immune system. For simplicity, the targeted vector without ELP will be shown as EDM-H2A-NLS- TM or namely <u>VT;</u> the vector equipped with ELP will be shown as <u>VET</u> and the vector with ELP but without targeting motif will be shown as VE. PC-3 prostate cancer cells are selected as target because they are highly metastatic and characterized to be $CAR^-/HER2^-$. This means that they are not a good candidate for adenoviral gene therapy or Herceptin anti-HER2 immunotherapy. Therefore, development of a targeted delivery system for this type of prostate cancer cells could be highly beneficial.

CAR: Coxsackie Adenovirus Receptor

HER2: Human Epidermal Growth Factor Receptor 2

<u>Body</u>

This is the final report; therefore, below we have highlighted the studies that have been conducted over the entire period of the DOD grant. We have met all the proposed objectives of Years 1-3. Four tasks were proposed for years 1 to 3:

Task 1- Biosynthesize and characterize recombinant vectors composed of EDM, Histone H2A, NLS, CS, ELP and TM (months 0-14).

1.1.   The genes encoding EDM-H2A-NLS-CS-ELP (VE), EDM-H2A-NLS-CS-ELP-TM (VET), and EDM-H2A-NLS-CS-TM (VT) will be synthesized and sequenced (months 0-2)

- The genes encoding VE, VET and VT were designed and sent to IDTDNA Inc.(Coralville, IA) for synthesis. The genes were synthesized and the correctness of sequences was confirmed by DNA sequencing.

1.2. The genes will be cloned into pET21b vector using standard cloning techniques and sequenced (months 2-4)

- All three genes were cloned into pET21b vector using standard cloning techniques and the sequences were verified.

1.3. The genes will be expressed and purified in *E. coli* expression system. The purity and expression levels will be confirmed by SDS-PAGE and westernblot analysis. The exact molecular weight and amino acid content will be determined by amino acid content analysis (Common Wealth biotechnologies Inc., Richmond, VA). (months 4-10)

- All three genes (i.e., VE, VET, and VT) were successfully expressed in *E.coli* and purified to >96% purity. The SDS-PAGE and Westernblot analysis of the expressed VT vector is shown in **Fig. 1** as an example. The expected molecular weight of the peptide is 23,631 daltons. A sample was sent to the Common Wealth Biotechnologies Inc. for amino acid content analysis. Unfortunately, due to the buffer intereference, no accurate measurements of the amino acid content could be performed. Nonetheless, the SDS-PAGE and westernblot analysis are sufficient to demonstrate the expression and purity of the vector.
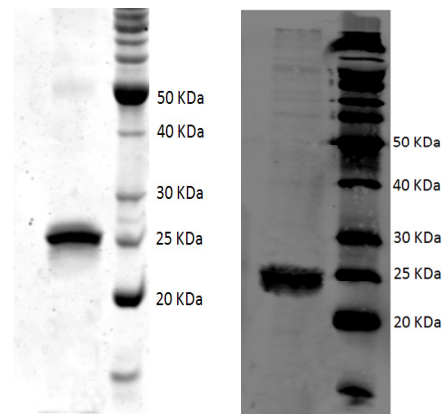

Fig. 1: SDS-PAGE (left panel) and westernblot (right panel) analysis of the purified VT vector. This figure confirms the high purity and expression of the vector.

1.4. The expression will be optimized and scaled up in 6L culture medium using various culture media and under different growth conditions (months 10-13).

- Owing to the highly basic nature of the vectors and toxicity to *E.coli* system, the challenge had to be addressed by successfully screening a stable expression host and optimizing the growth temperature, induction time and extraction and purification conditions. The suitable expression host was determined to be E. coli BL21(DE3) pLysS and the expression conditions of 30°C and 0.4mM IPTG. Also, the storage conditions and the desalting techniques were major challenges which were resolved successfully. We have reported these conditions for similar constructs in a recently published paper [1].

We currently have the complete protocol for the large scale production of all three vectors.

1.5.   The ability of cathepsin D in cleaving its substrate will be examined and optimized. A cell toxicity assay will also be performed (months 13-14).

- The ability of the cathepsin D in cleaving its substrate was verified. The method used to make this observation has previously been published by our group (Wang et al., J Control Release, 2009, PMID: 19303038).
- The results of the toxicity assay is presented below under task 2, section 2.2.

Task 2- Complex the vector with pDNA (i.e, pEGFP or pCM-Luc) to form nanocarriers and evaluate the transfection efficiency in vitro (months 14-24).

2.1. Vector/pDNA complexes will be formed and particles will be characterized under various physicochemical conditions including pH, temperature, and salt conditions. The nanoparticles will be stabilized and optimum conditions to form nanoparticles will be identified (months 14-17).

- The mean hydrodynamic particle size and charge of vector/pDNA complexes were determined using Dynamic Light Scattering (DLS) and Laser Doppler Velocimetry (LDV) respectively. All three vectors were able to complex with pDNA (pEGFP) and formed particles with sizes below 100nm. The particle size and charge analysis for VT is shown in **Fig. 2.** This method has previously been published by our group [1]. The particles demonstrated stability under various pH, temperature (up to $37^{o}C$) and salt concentrations (up to 150mM NaCl).
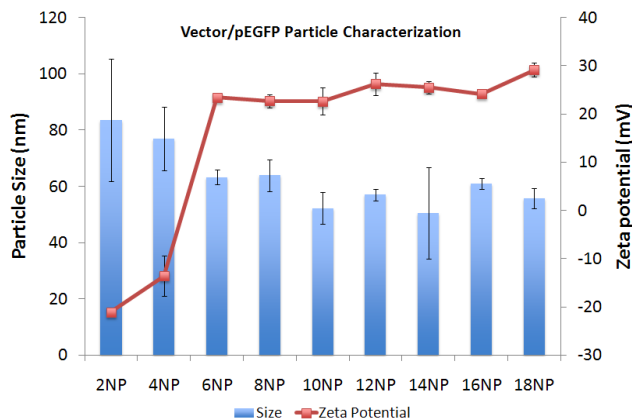
Fig. 2: Various amounts of vector in HEPES buffer were added to 1 μg of pDNA (pEGFP) to form complexes at different N:P ratios (N-atoms in vector to P-atoms in pDNA) in a total volume of 100μl deionized water. After 30 minutes of incubation, the size and zeta potential of the complexes were measured and reported as mean ± s.d., (n=3). Each mean is the average of 15 measurements and n represents the number of separate batches prepared for the measurements.

2.2. Cell transfection studies will be performed using PC-3 and RWPE-2 cells. Cells will be transfected with vector/pEGFP complexes at various N/P ratios in the presence and absence of chloroquine, bafilomycin, and Nocodazole and the transfection efficiency will be measured. The cell transfection process will be optimized to obtain highest transfection efficiency (months 17-24)

- Please note that we had originally proposed to use RWPE-2 normal prostate epithelial cells. However, through consultation with Dr. G. Meadows (collaborator at Washington State University) who is a cancer biologist we replaced it with RWPE-1 which is a more appropriate cell line and a better representative of normal human prostate cells.
- The transfection efficiency was optimized and the ability of the VT vector to target and transfect PC-3 prostate cancer cells but not RWPE-1 normal epithelial prostate cells is shown in **Fig. 3**. The details of the method of cell transfection have been previously published by our group [1].
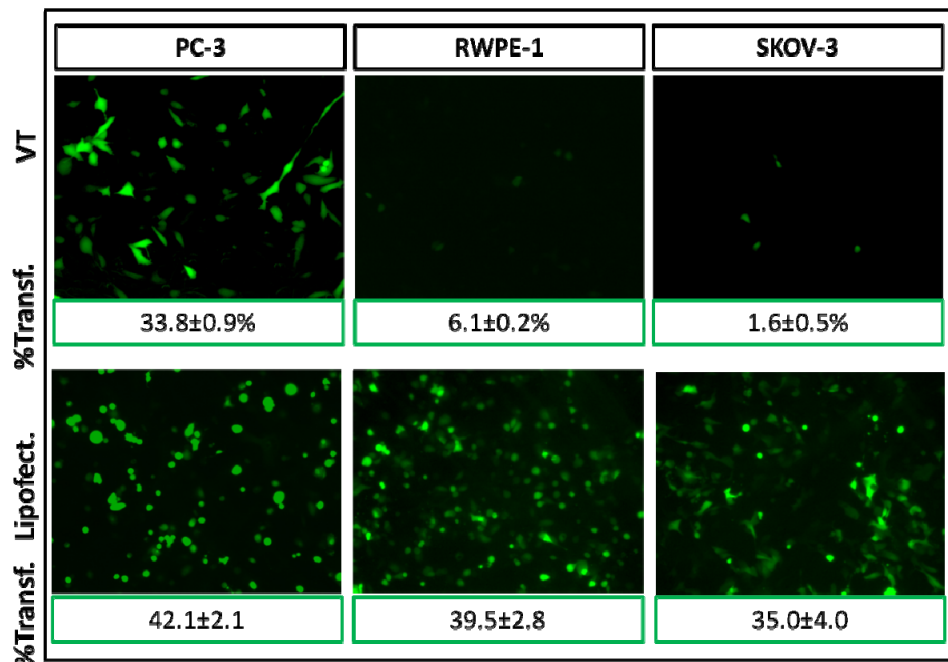
Fig. 3: Demonstration of PC-3 targeted gene delivery. Qualitative and quantitative representation of the PC-3 (CAR$^-$/HER2$^-$), RWPE-1 (normal cells) and SKOV-3 cells (CAR$^-$/HER2$^+$) transfected with VT/pEGFP complexes at N:P ratio of 10 and lipofectamine/pEGFP. The percentage of transfected cells is measured by flowcytometer. This figure shows that the VT vector can target and transfect prostate cancer cells while preserving normal cells. In contrast, commercially available vectors such as lipofectamine non-selectively transfect all cells which could result in unwanted toxicity to normal cells during the therapy.

- Using a WST-1 cell toxicity assay, the potential toxicity of the VT vector to PC-3 cancer cells was evaluated. The details of this method have previously been published [1]. We did not observe any vector related toxicity in PC-3 cancer cells at any NP ratio tested **(Fig. 4).** At NP ratio of 18, 23.5μg of vector is used to complex with 1μg of pEGFP.
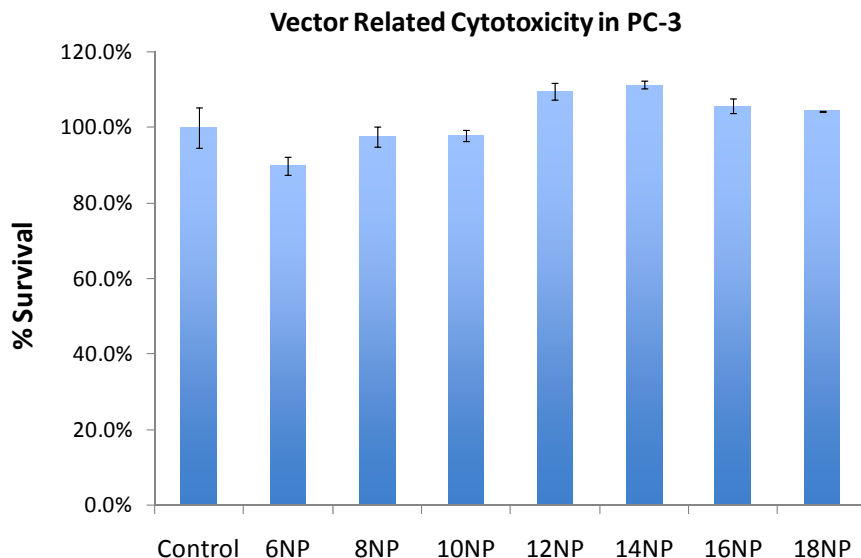
Vector Related Cytotoxicity in PC-3

Fig. 4: PC-3 cells were seeded at 10,000 cells/well in 96-well plates. Cells were transfected with VT/pEGFP complexes formed at various N:P ratios (equivalent to 1ug pEGFP). The control group received no treatment. 48 hours after transfection, a WST-1 (Roche Applied Science, Indianapolis, IN) cytotoxicity assay was performed to determine the vector related cytotoxicity in this cell line.

2.3. An animal protocol will be prepared and submitted for approval by the IACUC (months 22-24).

- The animal protocol was prepared and approved by the IACUC (Protocol #: 10-070). The approval from DOD Animal Care and Use Review Office (ACURO) was also obtained.

Task 3- Inject the nanocarriers in mice bearing xenograft tumor model of prostate cancer and evaluate the transfection efficiency and therapeutic efficacy (months 24-35).

3.1. To evaluate transfection efficiency, pCMV-luc or pEGFP will be complexed with vectors and used to transfect PC-3 tumors in nude mice. The transfection efficiency in tumors and other tissues will be evaluated using an in vivo imaging system. These studies will be performed using <u>40 nude mice</u>.

- To evaluate the ability of the vectors to reach PC-3 tumors and transfect cancer cells, first PC-3 tumors were implanted in the hind legs of nude mice (8mice/group). Group 1 received 100ul of saline, group 2 received of VE/pCMV-luc complexes (equivalent of 20ug pDNA that expresses luciferase), group 3 received VT/pCMV-luc complexes (20ug), group 4 received VT-VE mixture (50:50) in complexation with 20ug of pCMV-luc, and group five received pCMV-luc (20ug) alone. The result of this study showed that VT-VE mixture (50:50) in complexation with pCMV-luc had the highest rate of transfection efficiency in tumors (Figure 5D). This could be due to the presence of elastin shielding motif and targeting motif in the nanoparticles structures. The VE/pCMV-luc nanoparticles were also able to transfect tumor cells but with lower efficiency. This was most likely due to the lack of presence of targeting motif (Figure 5C). VT/pCMV-luc nanoparticles failed to reach tumors and transfected non-tumor tissues (e.g., lungs/liver) (Figure 5B). These nanoparticles were not shielded and as expected accumulated in lungs. No luciferase activity was observed in mice treated with pCMV-luc only and saline solution (Figure 5A, only pCMV-luc is shown).
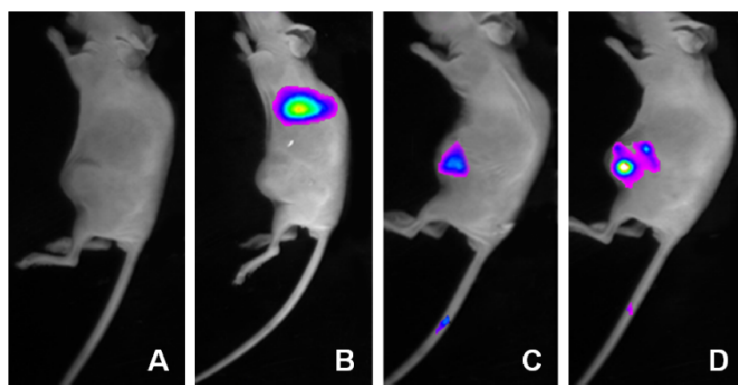

Figure 5: Luciferase expression detection in PC-3 tumor bearing nude mice using IVIS animal imaging system. Nude mice were injected with: A) pCMV-luc only, B) VT/pCMV-luc complexes, C) VE/pCMV-luc complexes, D) VE-VT/pCMV-luc complexes. The transfection efficiency was evaluated 24 hours post injection.

3.2. To evaluate therapeutic efficacy, Xenograft tumors of prostate cancer will be established in nude mice. The mice will be treated with vector/pSR39 complexes and controls. The size of tumors will be measured at various time points. Apoptotic activity of SR39 in tumor tissue versus normal tissues will be studied by TUNEL apoptotic assay.

- Based on the results shown in **Figure 5**, the ability of VT-VE vectors to transfect PC-3 tumors with SR39 gene (encodes mutant thymidine kinase) and result in tumor size reduction was evaluated. Thymidine kinase is an enzyme that converts non-toxic ganciclovir prodrug into its cytotoxic form. VT-VE/pSR39 complexes only, phosphate buffer saline (PBS) injection vehicle, prodrug ganciclovir (GCV), and plain pSR39 (uncomplexed) in combination with GCV were used as controls

(8mice/group). Using tail vein, mice were injected with VT-VE/pSR39 complexes on days 1, 5, and 10. The GCV administration started on day 2 and continued until day 15. The results showed significant tumor size reduction in mice treated with VT-VE/pSR39 complexes plus GCV (20 mg/kg/day).
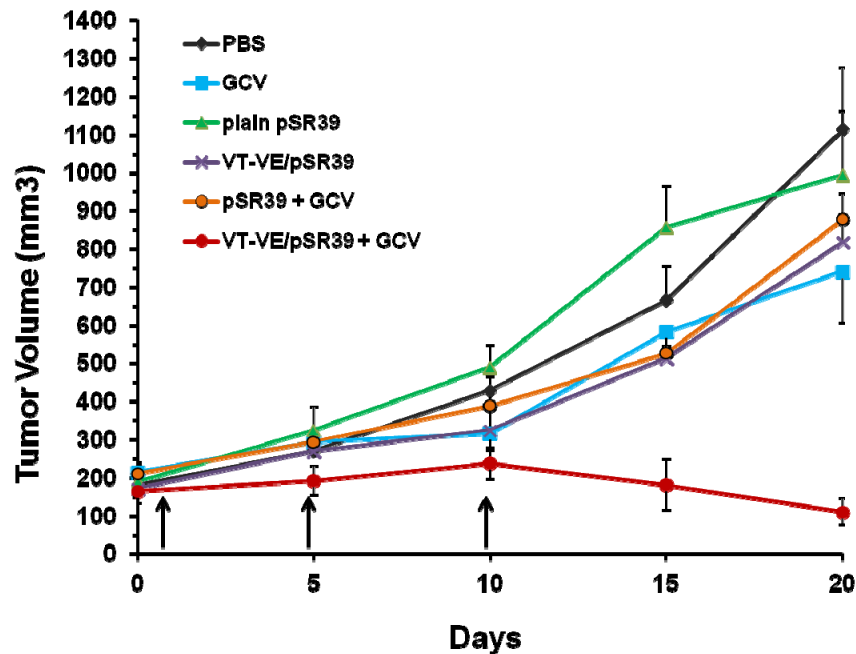
Figure 6: Evaluation of efficacy of VT-VE vectors to deliver pSR39 gene to PC3 bearing nude mice. 20ug of pSR39 was delivered each time on days 1, 5 and 10 followed by GCV administration. No significant tumor size reduction was observed in control groups.

Note: We did not perform Apoptotic TUNNEL Assay due to lack of funds.

Task 4- Evaluate immune system response to the nanocarriers using immune-competent mice (months 32-35). This task will be performed in the Department of Pharmaceutics Rooms 202-206 and vivarium at Rutgers University by the PI and the Postdoctoral Fellow in collaboration with Dr. Minko.

4.1. To test the immunogenicity of the vector, the production of anti-vector antibodies will be evaluated in mice. Intact male BALB/c mice will be given an intravenous injection of vector/pDNA nanocarriers or controls on days 7 and 21 after the initial challenge, for a total of two injections. The anti-vector antibodies will be assessed by ELISA. This study will be performed using immunocompetent mice (months 32-35).

- Male Balb/c mice (5-6 weeks old; Jackson laboratories; Maine, USA) were immunized via tail vein (i.v.) with the following formulations:

1- pCpG free plasmid only (1µg)
2- pBudce4.1 only (1µg plasmid DNA with CpG island)
3- Polyethyleneimine (synthetic polymer) in complex with 1µg pBudce4.1
4- PEGylated liposomes (prepared by our Collaborator Dr. Tamara Minko at Rutgers)
5- VT in complex with 1µg pBudce4.1
6- VET in complex with 1µg pBudce4.1

Nanoparticles were injected on Day 7 and Day 21. This dosing schedule was in accordance with previous studies conducted by Jain et al [2]. The study design is illustrated in the scheme below:

Mice arrive at vivarium; 5 weeks of age	Blood draw from Saphaneous vein; 200ul/mouse	Injection of nanoparticles	Injection of nanoparticles	Blood draw by cardiac puncture
↓	↓	↓	↓	↓

| Days | -7 | 0 | 7 | 21 | 35 |
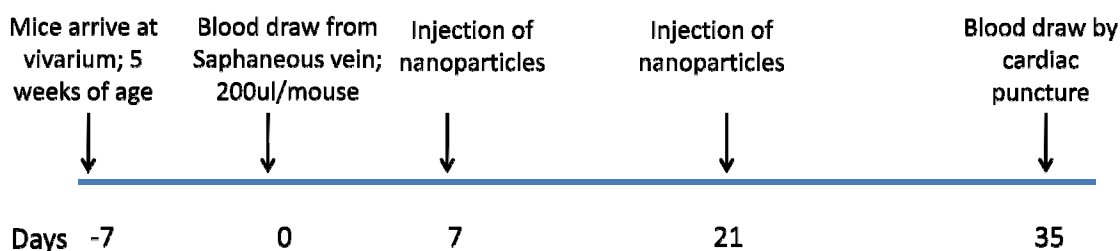
Briefly, Balb/c mice were housed for one week after arrival for acclamation (Day minus7). On Day zero, blood was collected after shaving the hair off by saphaneous vein puncture from both legs using a 3mm lancet (GoldenRod). Approximately 200ul of blood was collected in heparinized micro-Hematocrit tubes (Kontes). Blood from the capillary tubes were transferred to EDTA-coated microtainer tubes (BD). Plasma was collected by centrifugation of samples at 4000rpm for 20 minutes and stored at -80^0C until further evaluation. On day 7and day 21, animals were immunized via tail vein using a 27G needle with the nanoparticle formulations and controls as mentioned above. On day 35, animals were euthanized using CO_2 and blood drawn via cardiac puncture using a 25G needle. Blood was collected into EDTA-coated microtainer tubes (BD). Plasma was collected by centrifugation of samples at 4000rpm for 20 minutes and stored at -80^0C until further evaluation.

ELISA was performed to determine IgG and IgM levels as per manufacturer's instructions using the IgG and IgM ELISA kits from Bethyl laboratories.

The results of the experiments showed that neither VET nor VT induced production of IgG and IgM after repeated injections (**Figure 7**). This could be due to the fact that we used only 1ug of pDNA in our studies as a starting point. This amount of pDNA was chosen based on the published data by others [2]. In future studies, we will increase the amount of administered pDNA to 5ug and study the potential immune response.
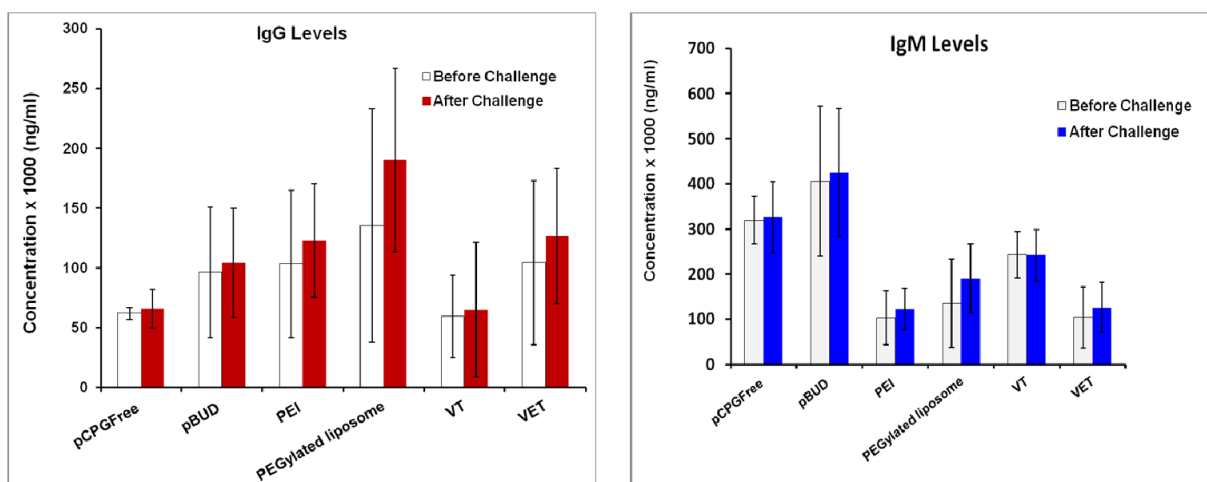
8

Figure 7: Immunogenicity studies for the evaluation of IgG and IgM production against antigens after repeated injections in immune-competent mice.

Task 5: Writing manuscripts, final report, and dissemination of the data in a conference (**Months 35-36**).

- We are in the process of preparing a comprehensive manuscript that includes the results of all the proposed studies.

Key Research Accomplishments
a) Developed stable nanoparticles with sizes less than 100nm. This size range makes them suitable for receptor-mediated endocytosis.
b) Formulated nanoparticles with ability to target PC-3 prostate cancer cells with high efficiency but with low binding to normal epithelial prostate cells.
c) A formulation of targeted shielded nanoparticles was screened with ability to target and transfect PC3 tumors but not other tissues.
d) The developed formulation could significantly transfect PC3 tumors after systemic administration and result in significant tumor size reduction.
e) Preliminary analyses of data obtained from the immunogenicity studies shows that our vectors are not immunogenic. However, more studies with larger doses need to be performed.

Reportable Outcome

A) **Manuscript:** The DOD Prostate Cancer Award was used to partially fund a closely related research project (reference 1). A copy of the manuscript is attached.   A   second   original research article is in preparation which includes all the results shown above.

B) Presentations:

1- The PI (A. Hatefi) received an invitation from the organizers of the Nanomedicine and Drug Delivery Symposium (NanoDDS'10) to give a talk about this research. This symposium was held on October 3-5, 2010 and the work was presented.

2- The PI (A. Hatefi) also submitted and abstract (Abstract#1847) and presented this work in DoD IMPaCT 2011 conference held in Orlando, Florida.

3- The PI (A. Hatefi) submitted an abstract and presented this work in Cancer Institute of New Jersey Annual Meeting (2012) held in Piscataway, NJ.

C) Training: A Research Scientist with experience in molecular biology techniques was hired. She received training in vector development, vector characterization, mammalian cell culture and transfection, and targeted prostate cancer gene therapy. In addition, two PhD students were trained to perform the studies.

D) Grant application: DOD Prostate Cancer Idea Award (2012)-Not funded.

E) Patent application: None.

Conclusions

Using genetic engineering techniques we have created a PC-3 specific gene delivery system that is able to accumulate in tumors and transfect prostate cancer cells but not non-tumor tissues. The gene delivery system is also able to deliver therapeutic genes to PC3 tumor cells efficiently and result in significant tumor size reduction. Preliminary immunogenicity results show that the vector does not induce production of IgG and IgM. It can be concluded that this system can *potentially* be used in the treatment of the patients that do not respond to adenoviral gene therapy or Herceptin immunotherapy.

References

[1]- Z. Karjoo, H. McCarthy, P. Patel, F. Nouri, **A. Hatefi,** Systematic Engineering of Uniform and Highly Efficient Targeted-Shielded Viral-Mimetic Nanoparticles. *Small* **(2013)** In press, PMID: 23468416

[2]- Anekant Jain, Weili Yan, Keith R. Millerc, Ronan O'Carrad, Jerold G. Woodwarde, Russell J. Mumper. Tresyl-based conjugation of protein antigen to lipid nanoparticles increases antigen immunogenicity. *Int J Pharm* 401 (2010) 87–92)
PMID: 20837122

<u>Appendices</u>

Appendix A: The Nanomedicine and Drug Delivery Symposium (2010) program highlights.

Appendix B: The published abstract for DOD IMPaCT 2011 conference.

Appendix C: The published abstract for Cancer Institute of New Jersey Annual Meeting (2012).

Appendix D: Reference 1

nanomedicine and drug delivery symposium -

October 3 - 5, 2010
Omaha, Nebraska

NanoDDS'10
omaha

Keynote Speakers
Joseph DeSimone (University of North Carolina at Chapel Hill)
Teruo Okano (Tokyo Women's Medical University)

Confirmed Speakers
Christine Allen (University of Toronto)
Mark Davis (California Institute of Technology)
Dennis Discher (University of Pennsylvania)
Iola Duarte (University of Aveiro)
Mohamed El-Sayed (University of Michigan)
Hamid Ghandehari (University of Utah)
Justin Hanes (The Johns Hopkins University)
Arash Hatefi (Washington State University)
W.E. Hennink (Utrecht University)
Leaf Huang (University of North Carolina at Chapel Hill)
Akihiro Kishimura (The University of Tokyo)
Philip S. Low (Purdue University)
Robert Luxenhofer (Dresden University of Technology)
Andrew Mackay (University of Southern California)
Muthiah Manoharan (Alnylam Pharmaceuticals)
Olivia Merkel (Philipps University, Marburg)
Xin Ming (University of North Carolina at Chapel Hill)
Tamara Minko (Rutgers University)
Randall Mrsny (University of Bath)
Vladimir Muzykantov (University of Pennsylvania)
Yukio Nagasaki (University of Tsukuba)
Derek O'Hagan (Novartis)
David Owen (Starpharma)
Robert Prud'homme (Princeton University)
Tom Redelmeier (Northern Lipids, Inc.)
Sonke Svenson (Cerulean Pharma Inc.)

Organizing Committee
Chair: Alexander Kabanov (University of Nebraska Medical Center)
Co-Chair: Tatiana Bronich (University of Nebraska Medical Center)
Christine Allen (University of Toronto)
Hamid Ghandehari (University of Utah)
Ralph Lipp (Eli Lilly & Company)
Christine Allmon (University of Nebraska Medical Center)
Marsha Fau (University of Nebraska Medical Center)
Keith Sutton (University of Nebraska Medical Center)

Registration and abstract submission: www.nanodds.org

nanomedicine and drug delivery symposium - omaha
NanoDDS'10

8th International Nanomedicine and Drug Delivery Symposium Omaha, NE, USA October 3-5, 2010

The field of nanomedicine has seen an exponential growth in the level of activity, investment, and development in recent years as evidenced by the creation of new companies, the launch of new scientific journals such as *Nature Nanotechnology*, *Nano Letters, and Nanomedicine-UK,* the establishment of new programs and departments in universities and government research institutions, as well as an extraordinary increase in the number of nanomedicine-focused publications. Developments in nanomedicine have already achieved true improvements in human health with the great promise of even more to come.   Drugs relying on delivery or formulation in nanotechnologies such as Doxil™ have been approved for human use while others like NK911, NK105, and SP1049C have entered clinical trial development.   Imaging agents for disease detection, characterization and staging such as Fenestra™ have also reached the late stages of pre-clinical development.   While nanomedicine now features prominently in many scientific meetings, conferences and symposia, the NanoDDS meeting series remains unique among them.

NanoDDS, now entering its eighth year, began in 2003 as a US-Japan mini-symposium organized by Dr. A. Kabanov and Dr. K. Kataoka. According to Dr. Ruth Duncan it was the first scientific meeting of its kind. NanoDDS has since established itself as an internationally-recognized, medium-sized and focused symposium highlighting new discoveries and developments in the field of nanomedicine while also serving as a forum to discuss the issues of pre-clinical and clinical development of nanomedicines. The intimate format of NanoDDS sets it apart from all other meetings of its kind, providing an excellent environment for interaction, networking, discussion, creativity and innovation between trainees (graduate students and post-doctoral fellows) and some of the world's leading academic scientists and industry specialists. These interdisciplinary interactions should aid in fostering new, fruitful collaborations,   leap-step advances, and ground-breaking discoveries.

SCIENTIFIC PROGRAM
Sunday October 3rd , 2010

First Keynote Presentation
Molecular Design of Intelligent Surfaces for Drug and Cell Delivery - *Teruo Okano, Tokyo Women's Medical University, Japan*

Session 1: Nanomedicines in Cancer (Part One)
Image Guided Design of Liposome-Based Cancer Therapy - *Christine Allen, Univ. of Toronto, Canada*

Ligand-Targeted Molecules for Imaging and Therapy of Cancer and Inflammatory Diseases
Philip S. Low,Purdue University

Nanotechnology Strategies to Overcome Limitations in Drug Delivery: Opportunities and Challenges - *Tamara Minko, Rutgers University*

Session 2: Nanomedicines in Cancer (Part Two)
Nanoparticle Delivery of siRNA for Cancer Therapy
Leaf Huang,University of North Carolina-Chapel Hill

Architectural Influence of Nanocarriers on Tumor Distribution and Toxicity
Hamid Ghandehari, University of Utah

From Concept to Clinic with Targeted Nanoparticles Containing siRNA
Mark E. Davis, California Institute of Technology

Session 3: Clinical Translation of Nanomedicines
Industrial Session and Roundtable - From Bench to Bedside: *Tom Redelmeier of Northern Lipids Inc., David Owen of Starpharma, Derek O'Hagan of Novartis, Sonke Svenson of Cerulean Pharma Inc., Muthiah Manoharan of Alnylam Pharmaceuticals*

Monday October 4th, 2010

Second Keynote Presentation
Engineering Better Medicines and Vaccines -*Joseph DeSimone, University of North Carolina-Chapel Hill*

Session Four: Novel Nanoformulation Technologies
Facile Production of Nanoparticles for Difficult to Deliver Therapeutics: hydrophobic drugs, peptides, and siRNA - *Robert Prud'homme, Princeton Univ.*

Novel Nanoparticles Functionalized for Anti-Oxidative Stress
Yukio Nagasaki, University of Tsukuba, Japan

Polymersomes to Filomicelles - thickness, shape, flexibility, charge...
Dennis Discher, University of Pennsylvania

Thermsensitive Polymeric Micelles for Tareted Delivery – *W. Hennink, Utrecht Univ., Netherlands*

Session Five: Tackling Nanomaterial–Tissue Interfaces to Improve Therapies and Diagnostics
Nanocarriers for Antioxidants
Vladimir Muzykantov, University of Pennsylvania

Strategies to Enhance Nanoparticle Transcytosis
Randall Mrsny, University of Bath, United Kingdom

The Mucus Barrier to Viral and Non-Viral Gene Therapy - *Justin Hanes, Johns Hopkins University*

Poster Sessions and Oral Presentations

Tuesday October 5th, 2010

Session 6: Nanomedicine Research Reports
Following Dynamic Biological Processes through NMR Spectroscopy and Metabonomic Profiling
Iola Duarte, University of Aveiro, Portugal

Customization of Genetically Engineered Vectors for Targeted Gene Transfer to Different Cancer Cells - *Arash Hatefi, Washington State University*

Novel polymeric hollow capsules "PICsomes"
Akihiro Kishimura, University of Tokyo, Japan

Doubly-Amphiphilic Poly(2-oxazoline)s with Unusual Microenvironment as High-Capacity Drug Delivery Systems - *Robert Luxenhofer, Dresden University of Technology, Germany*

Genetically Engineered Polypeptosomes
J. Andrew Mackay, Univ. of Southern California

SPECT Imaging of *in vivo* siRNA Delivery
Olivia Merkel, Philipps Univ.-Marburg, Germany

Molecular and Quantitative Pharmacology of siRNA Oligonucleotides Delivered via Receptor-Mediated Endocytosis - *Xin Ming, University of North Carolina at Chapel Hill*

Design and Evaluation of "Smart" Degradable Particles for Effective Gene Silencing
Mohamed E.H. El-Sayed, University of Michigan

GENERAL INFORMATION

Symposium Location
The symposium will be held at the Hilton Omaha, Nebraska's only 4 diamond hotel, located at 1001 Cass Street and within easy walking distance of the Old Market, Nebraska's premiere arts and entertainment district. The Hilton Omaha is only a short drive from Omaha's airport, as well as many other attractions including the Holland Performing Arts Center, Joslyn Museum, Durham Western Heritage Museum, and the Henry Doorly Zoo.

Accommodations
Accommodations are available at the Hilton Omaha at reduced conference rates.   Alternate accommodations may also be found at several nearby hotels. Please visit the symposium website www.nanodds.org for additional information.

Symposium Registration
To register for the symposium, or for additional information, please visit the symposium website www.nanodds.org.   Fees are $125 for graduate students and post-doctoral fellows, $400 for academics, and $1,200 for industry participants. These fees include admission to all three days of the symposium, an abstract book, name badge and conference packet, continental breakfasts, lunches, and refreshment breaks.

Call for Posters
The poster session will be the highlight of the symposium with time dedicated for poster viewing and discussion with the authors. A number of posters will be selected for oral presentations based on their scientific merit, innovation and clarity. Those interested in presenting their work during the poster session of the symposium should please visit www.nanodds.org for abstract submission guidelines and formats. Please email your abstract to nanodds@unmc.edu by Friday, August 27, 2010.

CONTACT
Questions about NanoDDS'10 may be directed to: nanodds@unmc.edu

www.nanodds.org

Abstract#1847: DEVELOPMENT OF A NANOTECHNOLOGY PLATFORM FOR PROSTATE CANCER GENE THERAPY

Arash Hatefi[1] and Yuhua Wang[2]

[1,2]Rutgers, The State University of New Jersey, Piscataway, NJ

[2]Washington State University, Pullman, WA

Background and Objectives: The objective of this research was to develop a multifunctional vector that can condense therapeutic genes into nano-size carriers, target PC-3 prostate cancer cells specifically and transfect and kill them efficiently. To achieve the objective, we developed a vector composed of four repeating units of histone H2A, a fusogenic peptide, and a PC-3 specific targeting motif. The PC-3 cancer cell model was chosen as a target because it represents a subpopulation of metastatic cancer cells that do not overexpress human epidermal growth factor receptor 2 (HER2) making them non-responsive to treatment with anti-HER2 antibodies such as Herceptin. In addition, PC-3 cells don't overexpress coxsackie adenovirus receptor which makes it a poor candidate for adenoviral gene therapy. Therefore, there is a need for the development a vector that can fill this gap and used for the treatment of such cancer cells.

Methodologies: The vector was designed, genetically engineered in Escherichia coli, and purified using nickel column chromatography. The vector was complexed with pEGFP (encodes GFP) and pTK (encodes thymidine kinase) to form nanosize particles. The size of the nanoparticles was measured using dynamic light scattering technique by Malvern Nano ZS90 instrument. Vector/pEGFP complexes were used to transfect PC-3 (prostate cancer), RWPE-1 (normal prostate), and SKOV-3 (ovarian cancer) cells. The transfection efficiency was determined using flow cytometry. The vector-related cytotoxicity was also determined by a WST-1 cell toxicity assay. To evaluate the therapeutic efficacy, the vector was complexed with pTK and used to transfect PC-3 cells. Concurrently, PC-3 cells received 25uM of ganciclovir (prodrug) for a period of 7 days. The killing efficiency of vector/pTK complexes was determined by WST-1 cell toxicity assay.

Results: The results demonstrated that the vector is able to condense plasmid DNA into particles with sizes less than 100 nm, target PC-3 cancer cells but not RWPE-1 or SKOV-3 cells, and mediate efficient gene expression. The cell toxicity assay data also showed that the vector by itself does not have any detectable toxicity at its maximum efficiency. The in vitro therapeutic efficacy studies revealed that the vector is able to kill approximately 70% of the PC-3 cells only in the presence of ganciclovir.

Conclusions: Recombinant DNA technology has allowed us to create a targeted multifunctional vector that can specifically kill PC-3 prostate cancer cells with minimal impact on normal prostate cells.

Impact Statement: The proposed nanosystem has a significant impact on prostate cancer gene therapy because it could fill the gap where immunotherapy and adenoviral gene therapy are not effective in treating patients with metastatic prostate cancer.

A Recombinant Non-Viral Vector for PC-3 Prostate Cancer Gene Therapy

Zahra Karjoo, Parin Patel, Faranak Salman Noori, Vidya Ganapathy, and Arash Hatefi

Department of Pharmaceutics, Rutgers University, Piscataway, NJ

Objectives: The objective of this research was to develop a multifunctional vector that can condense therapeutic genes into nano-size carriers, target PC-3 prostate cancer cells and transfect them efficiently. To achieve the objective, we developed a recombinant vector composed of four repeating units of histone H2A, a fusogenic peptide and a PC-3 targeting motif. The PC-3 cancer cell model was chosen as a target because it represents a subpopulation of aggressive prostate cancer cells with potential for metastasis. In addition, PC-3 cells don't express coxsackie adenovirus receptors which make them a poor candidate for adenoviral gene therapy.

Methodologies: The vector was designed, genetically engineered in E. coli and purified using nickel column chromatography. It was complexed with pEGFP (encodes GFP) to form nanosize particles. The size of the nanoparticles was measured using dynamic light scattering technique. Vector/pEGFP complexes were used to transfect PC-3 (prostate cancer) and RWPE-1 (normal prostate) cells. The transfection efficiency was determined using flow cytometry. The vector-related cytotoxicity was also determined by a WST-1 cell toxicity assay.

Results: The results demonstrated that the vector is able to condense plasmid DNA into particles with sizes less than 100 nm, target PC-3 cancer cells but not RWPE-1 and mediate efficient gene expression. The cell toxicity assay data also showed that the vector by itself does not have any detectable toxicity at its maximum efficiency.

Conclusions: Recombinant DNA technology allowed us to create a targeted multifunctional vector that can specifically transfect PC-3 prostate cancer cells with minimal impact on normal prostate cells. Using cancer suicide genes, the in vivo therapeutic efficacy studies are in progress.

Systematic Engineering of Uniform, Highly Efficient, Targeted and Shielded Viral-Mimetic Nanoparticles

Zahra Karjoo, Helen O. McCarthy, Parin Patel, Faranak Salman Nouri, and Arash Hatefi*

In the past decades, numerous types of nanomedicines have been developed for the efficient and safe delivery of nucleic acid-based drugs for cancer therapy. Given that the destination sites for nucleic acid-based drugs are inside cancer cells, delivery systems need to be both targeted and shielded in order to overcome the extracellular and intracellular barriers. One of the major obstacles that has hindered the translation of nanotechnology-based gene-delivery systems into the clinic has been the complexity of the design and assembly processes, resulting in non-uniform nanocarriers with unpredictable surface properties and efficiencies. Consequently, no product has reached the clinic yet. In order to address this shortcoming, a multifunctional targeted biopolymer is genetically engineered in one step, eliminating the need for multiple chemical conjugations. Then, by systematic modulation of the ratios of the targeted recombinant vector to PEGylated peptides of different sizes, a library of targeted–shielded viral-mimetic nanoparticles (VMNs) with diverse surface properties are assembled. Through the use of physicochemical and biological assays, targeted–shielded VMNs with remarkably high transfection efficiencies (>95%) are screened. In addition, the batch-to-batch variability of the assembled targeted–shielded VMNs in terms of uniformity and efficiency is examined and, in both cases, the coefficient of variation is calculated to be below 20%, indicating a highly reproducible and uniform system. These results provide design parameters for engineering uniform, targeted–shielded VMNs with very high cell transfection rates that exhibit the important characteristics for in vivo translation. These design parameters and principles could be used to tailor-make and assemble targeted–shielded VMNs that could deliver any nucleic acid payload to any mammalian cell type.

Z. Karjoo, P. Patel, F. S. Nouri, Dr. A. Hatefi
Department of Pharmaceutics
Rutgers University
160 Frelinghuysen Road, Piscataway, NJ, 08854, USA
Tel: +1-848-445-6366; Fax: +1-732-445-3134
E-mail: ahatefi@pharmacy.rutgers.edu

Dr. H. O. McCarthy
School of Pharmacy
Queen's University
Belfast, BT9 7BL, UK

DOI: 10.1002/smll.201300077

1. Introduction

In cancer gene therapy, for nucleic acid based drugs such as siRNA and plasmid DNA (pDNA) to reach their target sites, they must overcome several extracellular as well as intracellular barriers. In attempts to overcome these obstacles, multifunctional polymeric and lipid-based non-viral gene delivery systems (vectors) have been developed. These vectors are designed to protect nucleic acids from endonucleases by condensation into nanosize carriers, exploit the leakiness of tumor vessels and facilitate their accumulation in the tumor environment, enhance their internalization into the cancer

cells through use of targeting ligands and ultimately mediate efficient gene expression or knockdown. In order to extend the half-life and blood circulation time, the surfaces of gene carriers are usually decorated with highly hydrophilic polymers such as polyethylene glycol (PEG). The role of PEG is to sterically stabilize the surface of the nanoparticles, minimize interaction with plasma proteins (opsonization) and enhance the probability for accumulation in tumors via enhanced permeation and retention (EPR) effect.[1,2] PEG helps to achieve this goal by reducing the surface positive charge of the nanoparticles; thereby, minimizing the interaction with negatively charged blood components such as albumin and erythrocytes. Consequently, clearance by the mononuclear phagocyte system is significantly reduced.[3] Because the target sites of the nucleic acid delivery systems (e.g., siRNA and pDNA) are inside the cells, mere accumulation in the tumor environment is not enough and it is essential for the nanoparticles to be internalized by the cells. For this purpose, the nanoparticles also need to be equipped with targeting ligands (e.g., antibodies).[4] Therefore, an optimum balance of PEG to targeting ligand must be achieved on the surface of nanoparticles in order to reach maximum shielding without compromising internalization activity.

A number of PEGylated (shielded but non-targeted) drug delivery systems for small molecules (e.g., Doxil, Oncaspar) have reached the clinic, but no shielded and targeted delivery system for nucleic acid-based drugs has yielded such success. In fact, to date only one PEGylated and targeted formulation has reached Phase I clinical trials, namely CALAA-01.[5,6] One of the major reasons that has hampered the translation of nanotechnology-based cancer therapy into the clinic is the lack of delivery systems (vector) that are not only clinically safe and efficient but from manufacturing standpoint cost-effective and compliant with criteria for batch-to-batch uniformity.[7] A critically important consideration with regard to the design of PEGylated-targeted nanomedicines relates to the fact that many promising nanomedicines reported in the literature are multi-component and quite complex, and therefore difficult to synthesize and standardize by the pharmaceutical industry. Production of these multi-component systems involves several synthetic, purification and assembly steps. This increases the costs, complexity and batch-to-batch variation of such constructs and as a result significantly decreases their commercial attractiveness and clinical application.[8] Recently, during the Image-Guided Drug Delivery Summit organized by the National Institutes of Health (USA) the importance of simplicity in nanoparticle engineering and assembly process and batch-to-batch variation in relation to a final clinical product was notably highlighted as critical by a panel of scientists and physicians from industry and academia (Supporting Figure 1).[9]

Our lab in the past few years has demonstrated the possibility of creating targeted multifunctional (multicomponent) vectors in one step by using genetic engineering techniques. In this approach, the need for multiple conjugation/purification steps has been eliminated and the number of variables that needs to be optimized in structure/activity correlation studies reduced.[10–12] Utilizing this know-how, the objective of this research was to systematically engineer highly efficient targeted–shielded viral-mimetic nanoparticles (VMNs) with well-defined surface properties and uniform structure that can be made through an uncomplicated self-assembling process. To achieve the objective, we first genetically engineered a single chain multifunctional biopolymer that could overcome intracellular barriers by providing DNA condensation and internalization, endosome membrane disruption, nuclear localization and efficient gene expression. To overcome extracellular barriers and provide shielding, we then synthesized PEGylated histone H2A and adenovirus *Mu* peptides using a solid phase peptide synthesis approach. A library of VMNs with diverse physico-chemical properties was constructed as a result of complexation of pDNA with the multifunctional biopolymer in combination with PEGylated histone H2A or adenovirus *Mu* peptides. Through use of a series of physico-chemical and biological assays, the VMN library was screened in order to identify the constructs that are highly efficient, shielded, stable, bear an almost neutral surface charge and can be assembled in a reproducible fashion.

2. Results and Discussion

Numerous publications have previously explained the advantages of using recombinant techniques to synthesize fusion biopolymers allowing the production of biomacromolecules in a cost-effective manner.[13–15] In comparison to viral vectors and in terms of production costs, the recombinant biopolymers can be produced far cheaper than their viral counterparts. In addition, given the fact that multifunctional biopolymers can be synthesized/purified in one single step and that there is no need for the removal of toxic solvents or unreacted monomers, such recombinant multifunctional biopolymers could be just as, if not more cost-effective than their synthetic counterparts.[15]

To overcome the intracellular barriers, we genetically engineered a single chain multifunctional fusion biopolymer (vector) composed of a pH responsive fusogenic peptide (G), four repeating units of Histone H2A with an inherent nuclear localization signal (H) and a human epidermal growth factor receptor 2 (HER2) targeting affibody (T) (**Figure 1**A,B). Affibodies are small antibody mimetics composed of a three-helix bundle based on the scaffold of one of the IgG-binding domains of Protein A.[16,17] For simplicity, we refer to this vector as THG.

The major reason behind combining all four functional motifs into a single chain vector rather than four separate ones was to drastically reduce the number of variables that needs to be optimized in structure/activity correlation studies. As a result, the development process could be achieved in a shorter period of time. In a series of mechanistic studies, we previously demonstrated that all motifs in the THG vector are functional and it could efficiently transfect SKOV-3 HER2+ cancer cells.[12] As the THG vector could efficiently overcome the intracellular barriers, we used it as a base to formulate highly efficient targeted–shielded VMNs that could also overcome the extracellular barriers.

Firstly, the gene coding for THG was designed and optimized to be synthesized in an *E.coli* expression system. Western blot
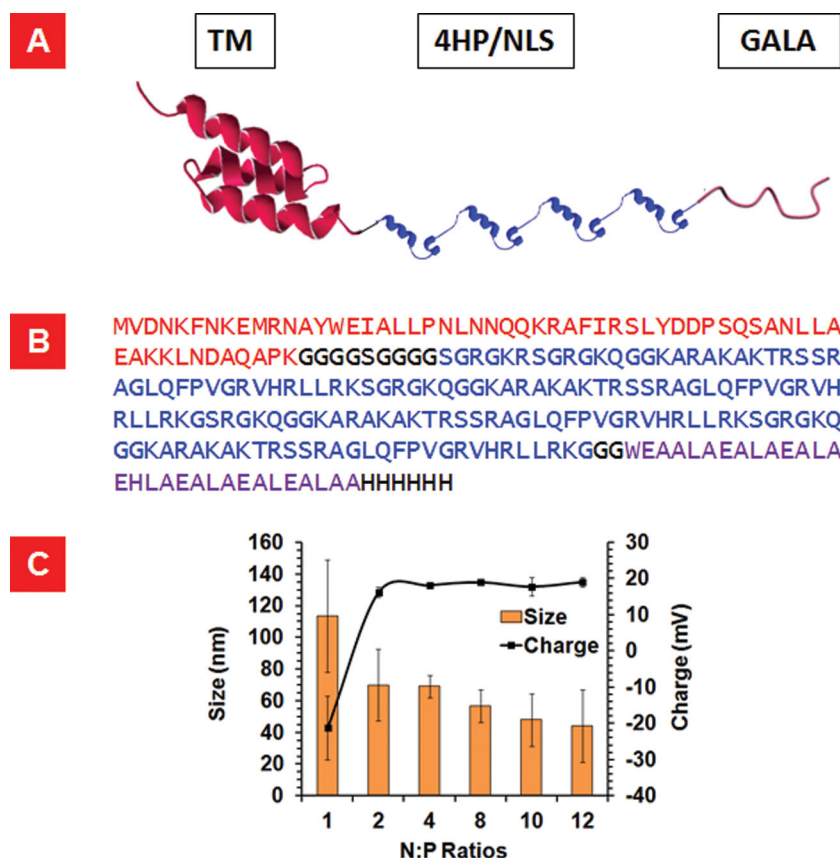
Figure 1. A) Schematic representation of THG recombinant vector composed of GALA (fusogenic peptide), four repeating units of histone H2A with an inherent nuclear localization signal (4HP/NLS) and a HER2 targeting motif (TM). The 3D structures of TM and Histone H2A are predicted using SWISS-MODEL program. B) The amino acid sequences of TM (red), 4HP/NLS (blue), and GALA (purple) in the THG vector. C) Particle size and charge analysis of THG in complex with pEGFP at different N:P ratios. The data are shown as mean ± s.d. (n = 3).

ious ratios to complex with pEGFP and form PEGylated-targeted VMNs (**Figure 2**). A series of physico-chemical and biological assays were then performed to characterize the assembled VMNs as explained below.

Firstly, we characterized the nanoparticles formed as a result of complexation of PEGylated peptides (e.g., H2A-PEG2K, H2A-PEG5K, etc.) and pDNA at various N:P ratios to evaluate their DNA condensation ability and particle surface charge. The results of the complexation studies showed that H2A-PEG2K, H2A-PEG5K, *Mu*-PEG2K and *Mu*-PEG5K in complexation with pEGFP can form nanoparticles with sizes of less than 100 nm and with almost neutral surface charges (Supporting **Figure 3**). At high N:P ratios (e.g., 10 or 12) where pDNA is fully condensed, the peptides that were PEGylated with PEG2K had on average significantly smaller sizes (ca. 20 nm) than peptides with PEG5K. This was expected as PEG5K has a larger molecular weight than PEG2K and could attribute to the increase in hydrodynamic particle radius. Furthermore, it could be observed that the presence of PEG did not interfere with the electrostatic interactions between peptides and pDNA and the nanoparticle formation process. In terms of zeta potential, the surface charge neutrality of these PEGylated nanoparticles is most likely related to the presence of PEG on the nanoparticles surface. Overall, the nanoparticle surface charge studies show that at one end of the spectrum the targeted non-PEGylated nanoparticles (THG/pEGFP) have a surface charge of ca. +20 mV (Figure 1C) while at the other end the PEGylated non-targeted nanoparticles (Supporting Figure 3) had surface charges of almost zero.
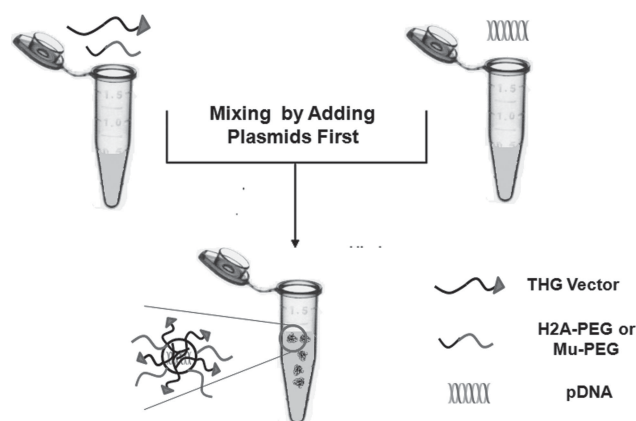
analysis and SDS-PAGE confirmed the expression and purity of THG protein (>95%) after Ni-NTA affinity chromatography (Supporting Figure 2). In the next step, the THG vector was desalted and used to complex with pDNA (pEGFP) to form targeted VMNs which were then characterized in terms of hydrodynamic particle size and charge. The results of this study showed that the sizes of the VMNs formed at N:P ratio of 2 or higher are below 100 nm and not statistically different from each other (*p* < 0.05) (Figure 1C). The desalting step is highly critical because it helps to remove the ions from the system and stabilize the particles' sizes by minimizing the potential for salt bridge formation in between nanoparticles and ensuing aggregation during storage time. The results of the zeta potential study revealed that the VMNs surface charge increased to a stable ca. +20 mV at N:P ratios 2 or higher (Figure 1C).

To stabilize and reduce the surface charge of targeted VMNs and incorporate shielding, we mixed the THG vector with two different PEGylated peptides (*i.e.*, H2A and *Mu*). These two peptides were purposely chosen because their efficient DNA condensation capabilities have previously been examined and reported.[18–19] PEG2K and PEG5K were covalently attached to H2A and *Mu* peptides to generate H2A-PEG2K, H2A-PEG5K, *Mu*-PEG2K and *Mu*-PEG5K. These peptides were used in combination with THG at var-

Figure 2. Schematics of PEGylated-targeted VMNs prepared through mixing of THG with H2A-PEG2K, H2A-PEG5K, *Mu*-PEG2K, or *Mu*-PEG5K followed by complexation with pDNA (pEGFP).
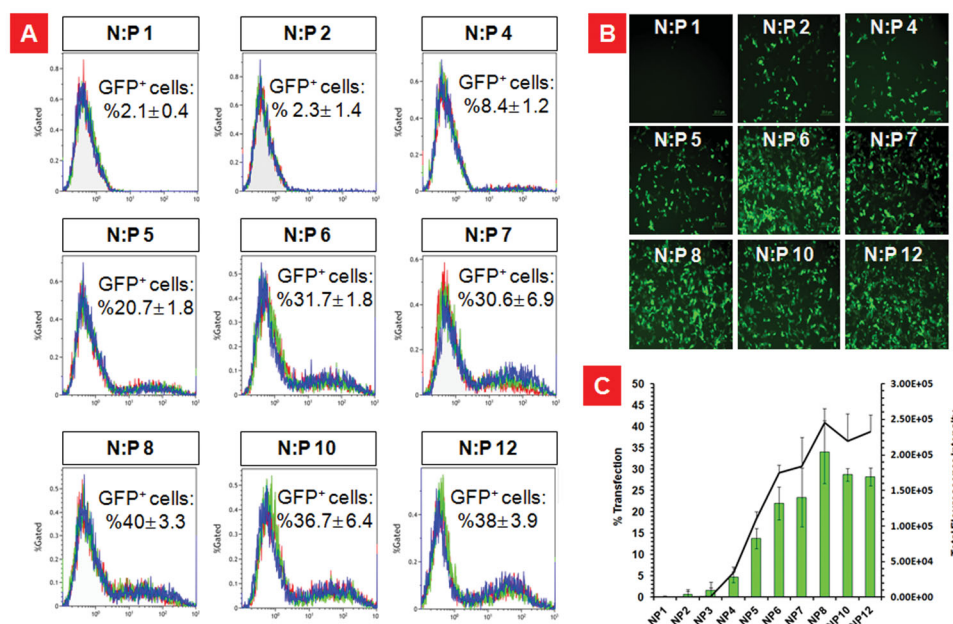
Figure 3. Evaluation of transfection efficiency of THG/pEGFP nanoparticles at N:P ratios of 1 to 12. A) Flowcytometry graphs showing the percentage of GFP positive cells. Each graph is an overlay of three independent repeats. B) Fluorescent microscopy images of the transfected SKOV-3 cells illustrating the extent of gene expression. C) A bar chart that quantitatively demonstrates the percentage of transfected cells and total green fluorescent protein expression. The data are shown as mean ± s.d. (n = 3).

To prepare targeted–shielded VMNs, various amounts of THG were mixed with PEGylated peptides at N:P ratios of 8, 10 and 12. These ratios were selected because this was the range that both targeted nanoparticles and PEGylated nanoparticles displayed maximum pDNA condensation. The results of the particle size and charge characterization study for targeted-PEGylated VMNs revealed that as the PEG content increased and THG content decreased, the nanoparticles surface charge gradually decreased from ca. +20 mV to −2 mV (Supporting Figures 4 and 5). This indicated that the PEG molecules could present themselves on the nanoparticles surface thereby reducing the VMNs surface charge. Overall, all the prepared nanoparticles had sizes between 40–100 nm which suggests that the presence of PEG2K and PEG5K in the nanoparticles did not interrupt the complexation process and all combinations were efficient in pDNA condensation. Nanoparticles in this size range (<150 nm) are known to be suitable for receptor mediated endocytosis as they can fit into clathrin-coated vesicles.[20]

Having a library of nanoparticles with known surface properties at our disposal, we investigated the ability of these PEGylated-targeted VMNs to internalize and transfect SKOV-3 cancer cells. This cell line was used as a model HER2+ mammalian cell line for this study because we have previously demonstrated that the affibody in the THG structure could recognize the HER2 on the surface of the cells and internalize (Supporting Figure 6).[12] In order to find the formulations of VMNs with the highest transfection efficiency, first we used THG/pEGFP nanoparticles at N:P ratios 1 to 12 to transfect cells. This was to determine the ratio at which the nanoparticles exhibit the maximum transfection efficiency. The results of the transfection studies showed that THG/pEGFP nanoparticles had maximum efficiency at N:P ratios of 8, 10, and 12 (Figure 3).

To examine the effect of PEG content in PEGylated-targeted VMNs on transfection efficiency, all the formulations of PEGylated-targeted VMNs that were prepared at N:P ratios of 8, 10 and 12 used to transfect SKOV-3 cells. For example, for N:P 8, all THG/PEGylated peptides combinations at weight/weight ratios of 12:0, 10:2, 8:4, 6:6, 4:8, 2:10 and 0:12 were examined. The weight/weight ratio of 12:0 indicates 12 µg of THG and 0 µg of PEGylated peptide (e.g., H2A-PEG2K or Mu-PEG5K, etc.), whereas weight/weight ratio of 0:12 indicates 0 µg of THG and 12 µg of PEGylated peptide. The general pattern of transfection efficiency demonstrated that particles with higher or equal amounts of THG to PEGylated peptide had higher transfection efficiency (weight/weight combinations of 10:2, 8:4, 6:6) in comparison to the nanoparticles with lower amount of THG (4:8, 2:10, 0:12), (**Figure 4**A–D).

The impact of PEG content was to an extent that none of the PEGylated nanoparticles (non-targeted) were able to transfect SKOV-3 cells. This is most likely due to the presence of PEG on nanoparticles surface which inhibits interaction between cell membranes and nanoparticles. Similar observations have previously been reported by other groups.[21] In contrast, a remarkably high rate of transfection efficiency (>%95) was observed with THG/Mu-PEG5K (8:8) at N:P ratio of 12. We believe that at this particular ratio the number of targeting peptides exposed on the nanoparticle surface is at the optimum density providing the ideal opportunity for the nanoparticles to interact with cells very effectively and internalize. It has previously been shown that there are an optimum number of ligands that should be present on the surface of each nanoparticle to achieve maximum efficiency.[22] Increasing ligand number yields a corresponding increase in receptor binding associated with increased avidity. However, above a certain level, this increased avidity could result in
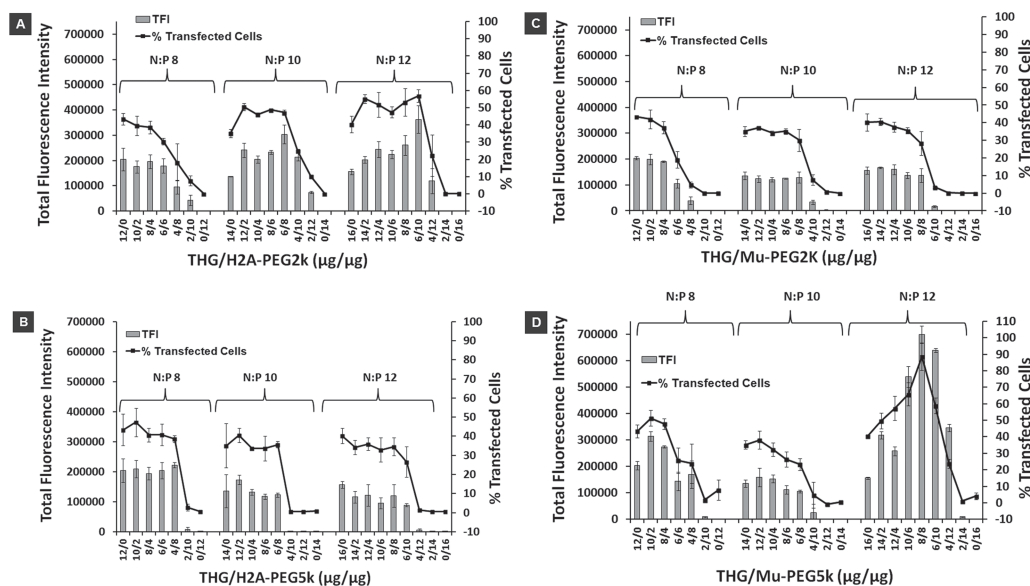
Figure 4. (A–D) Percentage of GFP-positive cells and total green fluorescent protein expression (TFI) for SKOV-3 cells transfected with vector/pEGFP complexes at various N:P ratios and in different combinations. The data are shown as mean ± s.d. (n = 10).

increased receptor down regulation due to endosomal sorting to lysosomes for degradation, resulting in a decreased number of receptors available for binding the vector. This concept has been elegantly shown in a study by Wagner et al. (1990) using transferrin conjugated onto polylysine.[23]

To examine whether formulation cytotoxicity was the cause of the low transfection in the cells, for example with THG/Mu-PEG5K (4:12) in comparison to THG/Mu-PEG5K (8:8), a cell toxicity assay was performed. This study was carried out on some of the most efficient nanoparticles prepared as a result of complexation of THG/Mu-PEG5K or THG/H2A-PEG2K with pEGFP. The results of the cell toxicity assay illustrated that none of the tested formulations were toxic ($p < 0.05$); and therefore, transfection efficiency was not negatively affected by the PEGylated-targeted VMN formulations (**Figure 5**). Previous studies with THG also showed

that the vector itself or complexed with pDNA had no significant impact on cellular viability most likely due to its biodegradability and low surface positive charge.[12,24]

The remarkably high efficiency of the THG/Mu-PEG5K (8:8) VMNs formed at N:P 12 prompted us to characterize them further in terms of shape and surface morphology and examine particle size uniformity. We adapted a previously published method for transmission electron microscopy (TEM) of viruses in order to study the surface morphology and internal structures of our formulated VMNs.[25] Brief staining was used to observe the surface morphology of the particles and the results showed that the prepared VMNs are somewhat floccus, uniform in size and spherical (**Figure 6**A). To investigate internal structures, the staining time was extended which helped to visualize the packaged pDNA inside VMNs. In this case, the condensed pDNA could be observed at the nanoparticle's core (Figure 6B).

For comparison's sake, we searched the literature to find clear TEM images of a model virus and compare with our VMNs. The results of the side-by-side shape comparison study illustrates that the surface morphology and internal structure of the formulated nanoparticles (Figure 6A–B and C right panel) are similar to poxvirus (Figure 6C, left panel). Overall, these observations show that the nanoparticle formation process could produce uniform, highly compact and spherical nanoparticles with similar morphology to viruses.

As mentioned in the introduction, apart from efficiency, a formulator needs to demonstrate that the formulation can be prepared in a reproducible fashion. To measure reproducibility (batch-to-batch uniformity) usually ten independent batches of each formulation is prepared in order to determine the coefficient of variation for polydispersity index (PDI). Given that particle size and particle size distribution directly impact upon gene transfection efficiency, production of nanoparticles with a reproducible PDI allows the formulator to obtain consistent and reliable transfection results. In addition, as no specific limit is set for the
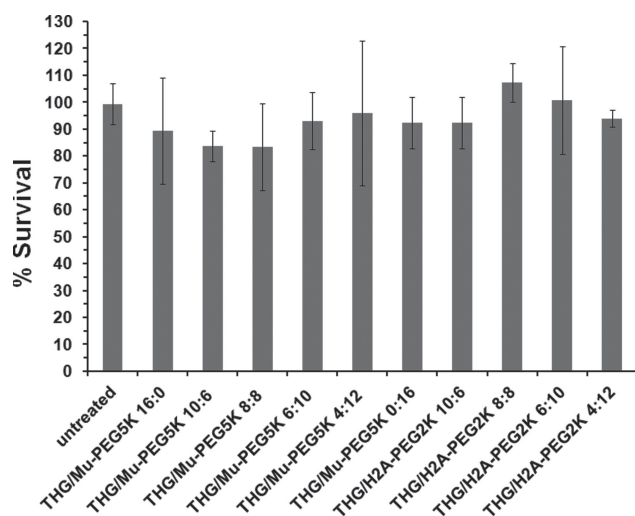

Figure 5. Evaluation of the viability of SKOV-3 cells after transfection with targeted and PEGylated- targeted VMNs. The data are shown as mean ± s.d. (n = 3).
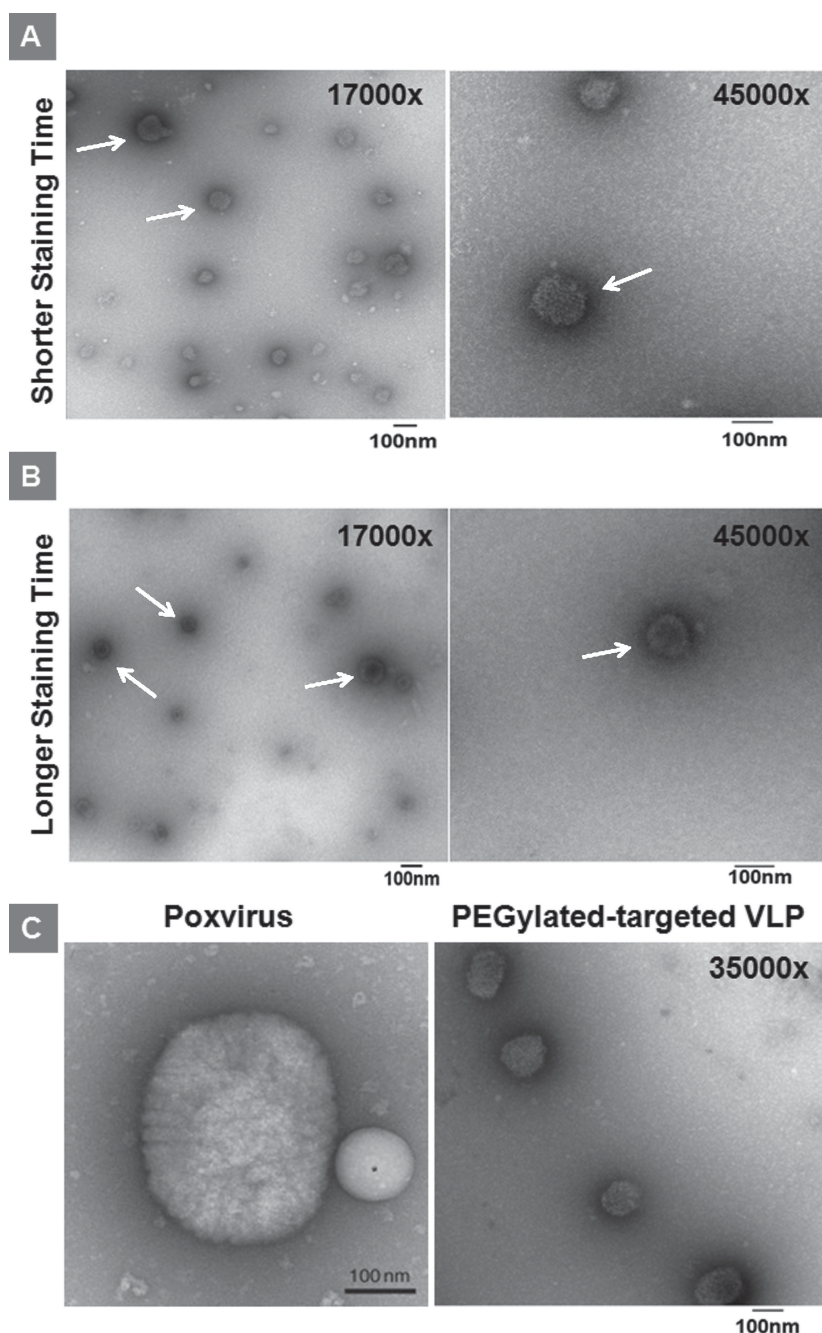
Figure 6. Transmission electron microscopy of the negatively stained targeted nanoparticles, PEGylated-targeted nanoparticles, and poxvirus. A) THG/pEGFP targeted nanoparticles stained briefly to emphasize on the representation of the surface structures. B) THG/pEGFP targeted nanoparticles with long staining times revealing internal structures. C) right panel: PEGylated-targeted VMNs formed as a result of complexation of THG/Mu-PEG5K (8:8) with pEGFP. left panel: poxvirus surface structure revealed as a result of negative staining. In this panel, a latex bead with a diameter of 100 nm is localized close to poxvirus. The poxvirus image is adapted with permission.[25] Copyright 2010, Elsevier.

(PEGylated liposome) but unfortunately do to the high costs (ca. $1500/vial) and serious shortage in the market this product was not used. To demonstrate reproducibility in VMN assembly process, we prepared ten independent batches of the VMNs through complexation of pEGFP with THG/Mu-PEG5K (8:8) or THG and evaluated the polydispersity index (PDI) and the corresponding CV. The results of the study demonstrated that the assembly process is reproducible because the coefficient of variation remained below 20% (**Figure 7**). As expected, Ambisome met the FDA requirements for batch-to-batch uniformity. It is worth emphasizing that for nanoparticles to be FDA approved they do not have to be perfect spheres or all of the same size. The nanoparticle formation process that is able to produce VMNs with statistically similar size distributions and efficacy is the critical factor. The results of our transfection studies (Figure 4), for example with THG/Mu-PEG5K (8:8) at N:P 12, also shows reproducibility in efficiency as the CV for ten repeats (n = 10) remained below 20%.

To avoid the complexities and stability problems associated with the long-term storage of nanosuspension formulations (e.g., aggregation), AmBisome is formulated as a dry product. A pharmacist or physician can simply add sterile buffer to AmBisome vial and reconstitute the formulation prior to usage. Following the same approach, the targeted THG vector and shielded Mu-PEG5K can be stored in one vial while the genetic material (pDNA) can be stored in another. A pharmacist or physician can simply add sterile buffer to each vial and mix the components of the two vials by simple shaking to make ready for injection VMN suspension. As a result, the need for long-term stabilization of the nanosuspension is eliminated and the suspension needs to remain stable and unaggregated only for a short period of time before injection. To examine the VMN stability after reconstitution, a particle stability study over time was performed and the data show that the formulated VMNs are stable for at least three hours with no statistically significant increase in size (**Figure 8**A).

The approaches that are commonly used in preparation of physically stable suspensions fall into two categories. One is the use of a vehicle to maintain deflocculated particles in suspension and the other is to apply the principles of flocculation to produce flocs that, although they settle rapidly, are

associated coefficient of variation (CV) for nanosuspensions by the FDA and it can vary from product to product (ranging from 15–25%), we used Ambisome as a control because it is an FDA approved nanotechnology-based product (non-PEGylated liposome) and currently available in the market. Another good control for this study would be Doxil
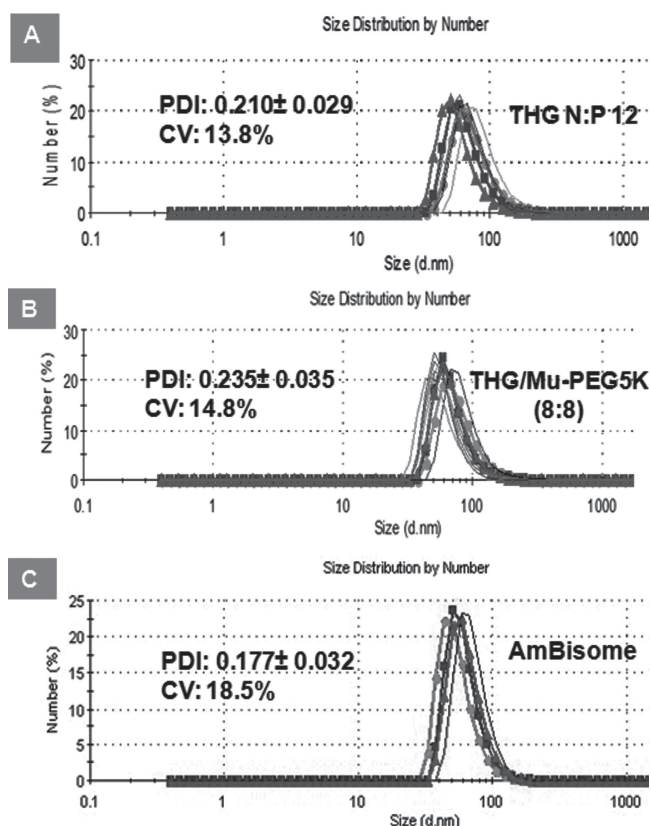
Figure 7. Polydispersity index analysis and measurement of coefficient of variation. A) Particle size distribution of THG/pEGFP at N:P 12. The data are shown as mean±s.d. (n = 10). B) Particle size distribution analysis of nanoparticles formed through complexation of THG/Mu-PEG5K (8:8) at N:P 12 with pEGFP. The data are shown as mean ± s.d. (n = 10). C) Particle size distribution of Ambisome. The data for Ambisome are shown as mean ± s.d. (n = 4).
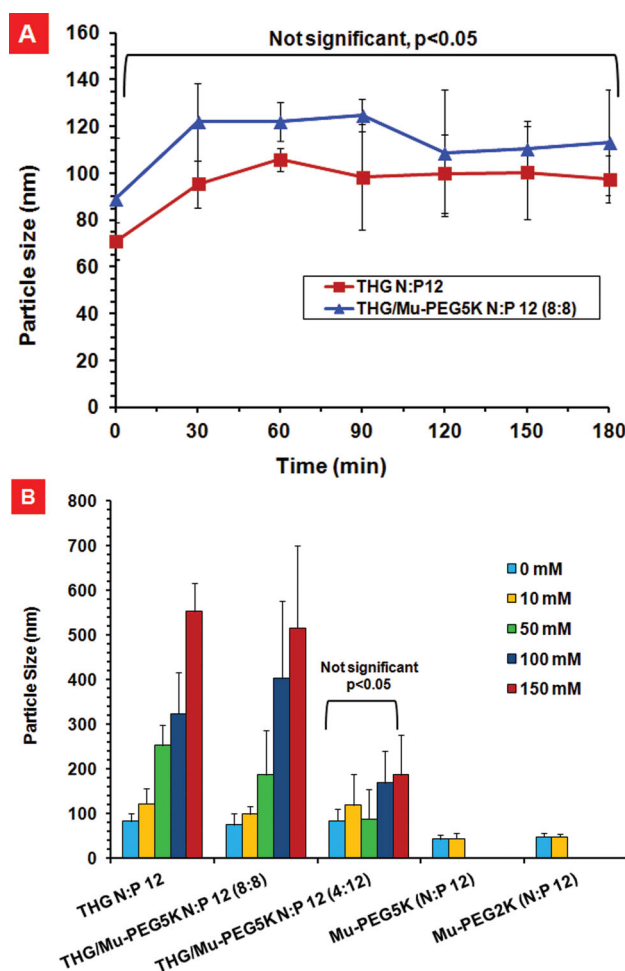

Figure 8. Particle size stability studies. A) Stability over time of the nanoparticles prepared through complexation of THG with pEGFP and THG/*Mu*-PEG5K (8:8) with pEGFP. B) Particle size stability at various salt concentrations. The data are shown as mean ± s.d. (n = 3).

easily resuspended with a minimum of agitation. Parenteral suspensions are usually formulated as deflocculated system in order to avoid potential clogging of arteries. The results in Figure 8A indicate that the nanosuspension is a deflocculated system because no significant size increase was observed over 3 h storage time.

In addition to storage time stability inside the vial before injection, the stability of the nanoparticles in the presence of salt at physiological concentrations (150 mM) and resisting dissociation is also important. Salt stability study is especially important for nanoparticles that are formed predominantly through electrostatic interactions because the presence of ions could easily interfere with the vector/pDNA attractive forces and result in particle dissociation.[26] For this purpose, the impact of salt concentration on the stability of the nanoparticles formed as a result of complexation of pDNA with THG/*Mu*-PEG5K (N:P 12, 8:8) which had the highest rate of transfection efficiency was studied. Other vectors such as THG (N:P 12), THG/*Mu*-PEG5K (N:P 4:12), *Mu*-PEG5K and *Mu*-PEG2K were also studied as controls. After exposing the nanoparticles to increasing concentrations of the NaCl (up to 150 mM), it was observed that the nanoparticles of *Mu*-PEG5K and *Mu*-PEG2K were not stable at salt

concentrations beyond 10 mM and rapidly dissociated at 50 mM NaCl or higher concentrations (Figure 8B). Basically, we could not detect any particles at high salt concentrations with these two peptides. In contrast, the THG/pEGFP (N:P 12) and THG/*Mu*-PEG5K (8:8) nanoparticles were stable in physiological salt concentrations (i.e., 150 mM), although we observed continuous increase in particle size as salt concentration increased. This size increase in the presence of salt was expected because it is known that salt ions could form salt bridges in between nanoparticles and result in formation of loose floccules.[27] It is noteworthy that after injection into the body, the VMNs will get diluted in the blood stream and as long as they don't dissociate, the potential for aggregation is very low. Nonetheless, there is a possibility for these VMNs to loosely interact with negatively charged plasma proteins because of their slightly positive surface charge. This prompted us to also examine the stability of the VMNs created through complexation of pEGFP with THG/*Mu*-PEG5K (4:12) which bears an almost neutral surface charge (Supporting Figure 5F). At this ratio, the nanoparticles contain significant amount of PEG and are expected to resist

aggregation. As it can be observed in Figure 8B, these nano-particles not only resisted aggregation but also dissociation. One factor that may have contributed to the salt stability of the THG-containing VMNs and resisting dissociation is the presence of hydrophobic residues in the THG sequence. These hydrophobic residues could contribute to the stabilization of hydrophobic pockets in the nanoparticle structure and block the penetration of water and ions into the nanoparticle core. As a result, the salt ions may have difficulty interfering with the electrostatic interactions in between pDNA and vector's cationic residues.

Based on all the observed results, VMN formulations with different physicochemical properties are at hand which could potentially demonstrate different pharmacokinetic profiles in vivo. Although the in vitro results suggest that THG/*Mu*-PEG5K (8:8) at N:P ratio of 12 may be the most efficient formulation, ultimately it is in vivo studies that will determine which formulation is the most effective at reaching tumors and transfecting cancer cells. This is due to the fact that in tumor targeting, at first the targeting is achieved via the EPR effect which is a form of passive targeting.[28]

3. Conclusion

Recent discussions among scientists in the academic and pharmaceutical industry indicate that pharmaceutical biotechnology companies face a significant challenge in making multicomponent targeted and shielded nanomedicines that are cost effective, stable and compliant with batch-to-batch uniformity.[9] This non-compliance appears to stem from the excessive number of chemical conjugation steps and the limited control over the reactions involved in the attachment of various functional moieties such as targeting ligands (antibodies) and shielding motifs (PEG) and subsequent formulation development for long-term stabilization of the nanosuspensions.

Overall, our results provide design parameters for engineering uniform targeted–shielded VMNs with high cell transfection rate that exhibit the important characteristics for in vivo translation. These design parameters and principles could be used to tailor-make and assemble targeted–shielded VMNs that could deliver any nucleic acid payload to any mammalian cell type.

In an attempt to ensure biodegradability and homogeneity, all components in VMN construct are amino acid based. As we utilized recombinant DNA technology to create a multifunctional biopolymer (THG) in a single step, the need for conjugation of various biological motifs to the vector backbone in multiple steps was eliminated. Here, we tried diligently to embrace the phrase coined by Prestwich which states "embrace complexity, engineer versatility, and deliver simplicity".[29]

4. Experimental Section

Production of THG Recombinant Vector: The gene encoding the THG vector was synthesized by IDT integrated DNA technologies with N-terminal *NdeI* and C-terminal *XhoI* restriction sites.

A C-terminal 6×histidine tag was also designed in the vector sequence to facilitate purification. The THG gene was then cloned into a pET21b expression vector (Novagen) and transformed into *E.coli* BL21 (DE3) p*LysS*. One BL21(DE3) plysS colony bearing THG-hisx6:pET21b was inoculated in 5 mL Circlegrow medium supplemented with Carbenicillin (50 ug/mL). The culture was incubated overnight at 30 °C. The day after, 5 mL overnight culture was added to 500 mL of Circlegrow medium and was shaken to reach OD_{600}>0.5. IPTG was added to final concentration of 0.4 mM and the incubation was continued for 6 h at 30 °C. Under these conditions the THG vector is expressed in soluble form. Cells were then collected at 5000*g* for 20 min. For the purification, 20 mL lysis buffer (5 M Urea, 1 M NaCl, 100 mM NaH2PO4, 10 mM Tris, 1% Triton X-100 and 10 mM imidazole, pH 8) per gram of cell pellet was added and the solution was stirred for 1 h followed by centrifugation at 37 000*g* for 1 h at 4 °C. Addition of 5 M urea to the lysis buffer increases the yield of the purification process by enhancing the exposure of histag to the nickle resins. The supernatant was collected and added to 1 mL Ni-NTA agarose (Qiagen) pre-equilibrated with lysis buffer. The slurry was shaken for 1 h on ice then added to the column. The column was washed with 100 mL of lysis buffer and 40 mL of wash buffer (5 M Urea, 1 M NaCl, 100 mM NaH2PO4, 10 mM Tris and 40 mM imidazole, pH 8). The protein was eluted by Elution buffer (3 M Urea, 500 mM NaCl, 100 mM NaH2PO4, 10 mM Tris and 200 mM imidazole, pH 8) and stored at −20 °C.

Desalting and Preparation of THG Stock Solution: A working stock of THG solution was prepared by passing the purified protein through Sephadex G-25 prepacked column (PD-10, GE Heathcare). The column was first conditioned with bis-tris propane buffer (10 mM, pH 7) plus NaCl (5 mM). Then the THG solution was loaded onto the column followed by washing the column with bis-tris propane buffer (10 mM, pH 7) plus NaCl (5 mM). The desalted THG solution was collected and the concentration of protein was measured by Nanodrop 2000 spectrophotometer (Thermoscientific) using molecular weight (27.62 kDa) and extinction coefficient (i.e., 13980) of the peptide.

Preparation of Targeted and PEGylated-Targeted VMNs: To prepare VMNs, total amounts of vector needed for a given N:P ratio was calculated. To prepare targeted VMNs, predetermined amounts of THG vector in HEPES buffer (100 mM, pH 7.4) were flash mixed with 1 µg of pDNA (pEGFP) to form complexes at different N:P ratios (1 to 12) in a total volume of 100 µL. Flash mixing (flash nanoprecipitation) means addition of peptide solution to pDNA solution in an instant. For example, to prepare N:P ratio of 1, 1.3 µg of THG vector was used to complex with 1 µg of pEGFP.

To prepare PEGylated-targeted VMNs, first truncated Histone H2A (H2A) with the amino acid sequence of RGKQGGKARAKAKTRSS-RAGLQFPVGRVHRLLRKGG and adenovirus *Mu* peptide with amino acid sequence of MRRAHHRRRRASHRRMRGG with >98% purity were synthesized by American Peptide Company (Sunnyvale, CA). Then, the synthesized peptides were PEGylated by using 2000 and 5000 dalton PEGs to make: H2A-PEG2K, H2A-PEG5K, *Mu*-PEG2K and *Mu*-PEG5K. The covalent conjugation of PEG to C-terminus of the *Mu* and H2A peptides were conducted by the American Peptide Company. A mix of THG with H2A-PEG2K, H2A-PEG5K, *Mu*-PEG2K and *Mu*-PEG5K at different weight/weight (µg/µg) ratios was prepared and complexed with pEGFP to make PEGylated-targeted VMNs. For example, at N:P 12, THG, and PEGylated peptides were

mixed at weight/weight ratios of 16:0, 14:2, 12:4, 10:6, 8:8, 6:10, 4:12, 2:14 and 0:16. The schematics of the method are shown in Figure 2.

Particle Size and Charge Analysis and Evaluation of Reproducibility: Targeted and PEGylated-targeted VMNs were prepared as described above and the mean hydrodynamic particle size and zeta potential of the particles were measured at room temperature using Nano-ZS Zetasizer (Malvern Instruments, U.K). The data are presented as mean ± s.d (n = 3). While for routine particle size and charge measurements the number of prepared independent batches was set at 3, for reproducibility measurements the number of samples was set at 10 (n = 10). Ambisome vials (n = 4) were kindly provided as a gift by the pharmacy store at the Cancer Institute of New Jersey (New Brunswick, NJ). To measure reproducibility, the average and standard deviation of polydispersity index (PDI) of ten samples was determined by the zetasizer and from that we calculated the coefficient of variation (CV) using the following formula: CV = standard deviation/mean × 100

Particle Shape Analysis by Transmission Electron Microscopy: To study the shape of the VMNs, one drop of sample was put on a carbon type B coated copper grid (Ted Pella, USA) for 5 min. The sample was dried and the grid was stained for 1–3 min depending on the need with 1% sodium phosphotungstate solution. The grids were imaged using transmission electron microscope (1200EX electron microscope, JEOL, USA) at RUMDNJ TEM core imaging facility. This method was adapted with slight modifications from a previously published method for imaging viruses.[25]

Particle Stability over Time and in the Presence of Salt: To measure the stability of the VMNs over time, the particle size measurements were performed every 30 min on each sample for 180 min. For particle stability studies in the presence of salt (NaCl), VMNs were prepared in HEPES buffer (pH 7.4) and considered as zero molar salt. From a 2 M NaCl stock solution, aliquots were taken and added to the VMNs in HEPES buffer until the desired NaCl concentration was obtained. The particle sizes at each salt concentration was measured and reported as mean ± s.d. (n = 3).

Cell Transfection Studies: The above mentioned VMNs were used to transfect SKOV-3 ovarian cancer cells using the previously reported methods.[24] The transfection protocol is similar to what is set as a standard for transfecting cells with viruses which are targeted nanoparticles with sizes less than 100 nm. For more information please see the standard protocol of cell transfection with adenovirus from MP Biomedicals (Solon, Ohio). In brief, SKOV-3 cells were seeded in 96-well plates. Cells were transfected with vector/pEGFP complexes at various N:P ratios (equivalent of 1 μg pDNA). The green fluorescent protein (GFP) was visualized using an epifluorescent microscope to evaluate GFP gene expression. To quantify transfection efficiency, percent GFP+ cells and total green fluorescence intensity was measured using F500 Flow Cytometer (Beckman Coulter, USA). Each time 10 000 cells were counted and the total fluorescence intensity of GFP+ cells was normalized against the total fluorescence intensity of untransfected cells (background control).The data are presented as mean ± s.d., (n = 10). Percentage of GFP+ cells was determined by Kaluza flow analysis software (Beckman Coulter, USA) using 99% gating. Total green fluorescence intensity (TFI) which is a measure of green fluorescent protein expression was calculated using the following formula: TFI = mean fluorescence value of each GFP+ cell (measured by flowcytometer) × total number of transfected GFP+ cells.

Cell Viability Study: SKOV-3 cells (4×10^4 per well) were seeded in a 96-well plate and incubated in McCoy's 5A full media. 24 h later, 100 μL of freshly prepared vector/pEGFP was added to each well. The cells were incubated with the VMNs for 2 h. Then the medium was replaced with fresh McCoy's 5A media. The cells were incubated at 37 °C for another 48 h, before WST-1 cell proliferation reagent (Roche Applied Science, Indianapolis, Indiana) was added to each well. The absorbance at 450 nm was measured 2 h after adding the reagent. Considering the viability of untreated cells as 100%, the viability of other samples was reported accordingly. The data are reported as mean ± s.d. (n = 3).

Supporting Information

Supporting Information is available from the Wiley Online Library or from the author.

Acknowledgements

[1] V. P. Chekhonin, Y. A. Zhirkov, O. I. Gurina, I. A. Ryabukhin, S. V. Lebedev, I. A. Kashparov, T. B. Dmitriyeva, *Drug Deliv.* **2005**, *12*, 1.

[2] J. Senior, C. Delgado, D. Fisher, C. Tilcock, G. Gregoriadis, *Biochim. Biophys. Acta* **1991**, *1062*, 77.

[3] F. Verbaan, I. van Dam, Y. Takakura, M. Hashida, W. Hennink, G. Storm, C. Oussoren, *Eur. J. Pharm. Sci.* **2003**, *20*, 419.

[4] J. Gao, J. Sun, H. Li, W. Liu, Y. Zhang, B. Li, W. Qian, H. Wang, J. Chen, Y. Guo, *Biomaterials* **2010**, *31*, 2655.

[5] M. E. Davis, *Mol. Pharmaceut.* **2009**, *6*, 659.

[6] M. E. Davis, J. E. Zuckerman, C. H. Choi, D. Seligson, A. Tolcher, C. A. Alabi, Y. Yen, J. D. Heidel, A. Ribas, *Nature* **2010**, *464*, 1067.

[7] T. M. Allen, P. R. CuCullis, *Adv. Drug Deliv. Rev.* **2012**, DOI: 10.1016/j.addr.2012.09.037.

[8] T. Lammers, F. Kiessling, W. E. Hennink, G. Storm, *J. Control. Release* **2012**, *161*, 175.

[9] P. Tandon, K. Farahani, *Cancer Res.* **2011**, *71*, 314.

[10] B. F. Canine, Y. Wang, A. Hatefi, *J. Control. Release* **2009**, *138*, 188.

[11] S. S. Mangipudi, B. F. Canine, Y. Wang, A. Hatefi, *Mol. Pharm.* **2009**, *6*, 1100.

[12] Y. Wang, S. S. Mangipudi, B. F. Canine, A. Hatefi, *J. Control. Release* **2009**, *137*, 46.

[13] Z. Megeed, H. Ghandehari, in *Polymeric Gene Delivery: Principles and Applications* (Ed: M. Amiji), CRC Press, Boca Raton, FL, USA **2005**, pp.489–507.

[14] H. Ghandehari, A. Hatefi, *Adv. Drug Deliv. Rev.* **2010**, *62*, 1403.

[15] B. F. Canine, A. Hatefi, *Adv. Drug Deliv. Rev.* **2010**, *62*, 1524.

[16] A. Orlova, M. Magnusson, T. L. Eriksson, M. Nilsson, B. Larsson, I. Hoiden-Guthenberg, C. Widstrom, J. Carlsson, V. Tolmachev, S. Stahl, F. Y. Nilsson, *Cancer Res.* **2006**, *66*, 4339.

[17] P. A. Nygren, *FEBS* **2008**, *275*, 2668.

[18] M. Keller, T. Tagawa, M. Preuss, A. D. Miller, *Biochemistry* **2002**, *41*, 652.

[19] D. Balicki, C. D. Putnam, P. V. Scaria, E. Beutler, *Proc. Natl. Acad. Sci. USA* **2002**, *99*, 7467.

[20] J. Rejman, V. Oberle, I. S. Zuhorn, D. Hoekstra, *Biochem. J.* **2004**, *377*, 159.

[21] M. C. Deshpande, M. C. Davies, M. C. Garnett, P. M. Williams, D. Armitage, L. Bailey, M. Vamvakaki, S. P. Armes, S. Stolnik, *J. Control. Release* **2004**, *97*, 143.

[22] C. M. Varga, T. J. Wickham, D. A. Lauffenburger, *Biotechnol. Bioeng.* **2000**, *70*, 593.

[23] E. Wagner, M. Zenke, M. Cotten, H. Beug, M. L. Birnstiel, *Proc. Natl. Acad. Sci. USA* **1990**, *87*, 3410.

[24] Y. Wang, B. F. Canine, A. Hatefi, *Nanomedicine* **2011**, *7*, 193.

[25] M. Laue, *Methods Cell Biol.* **2010**, *96*, 1.

[26] X. Zhang, M. R. Servos, J. Liu, *J. Am. Chem. Soc.* **2012**, *134*, 9910.

[27] A. B. Fall, S. B. Lindstrom, O. Sundman, L. Odberg, L. Wagberg, *Langmuir* **2011**, *27*, 11332.

[28] M. Yokoyama, *J. Artif. Organs* **2005**, *8*, 77.

[29] G. D. Prestwich, *Organogenesis* **2008**, *4*, 42.